Eleven-vertex *isocloso* Type Rhodaundecaboranes: Crystal Structures and Nuclear Magnetic Resonance Properties of $[(PMe_2Ph)_2RhHB_{10}H_8(OMe)_2]$ and $[(PMe_2Ph)_2RhHB_{10}H_8Cl(OMe)]$ *

Hayat Fowkes, Norman N. Greenwood, John D. Kennedy, and Mark Thornton-Pett
Department of Inorganic and Structural Chemistry, University of Leeds, Leeds LS2 9JT

The reaction between $[RhCl_3(PMe_2Ph)_3]$ and *closo*-$[B_{10}H_{10}]^{2-}$ in refluxing MeOH gives $[1,1\text{-}(PMe_2Ph)_2\text{-}1,2\text{-}\mu\text{-}H\text{-}2,5\text{-}(OMe)_2$-*isocloso*-$1\text{-}RhB_{10}H_8]$ as a bright yellow air-stable compound in low yield. Crystals are triclinic, space group $P\bar{1}$ with a = 948.8(4), b = 1 675.5(6), c = 1 855.0(6) pm, α = 101.48(3), β = 99.55(3), γ = 99.82(3)°, and Z = 4. An occasional by-product of the reaction is the yellow compound $[1,1\text{-}(PMe_2Ph)_2\text{-}1,2\text{-}\mu\text{-}H\text{-}2\text{-}Cl\text{-}5\text{-}OMe$-*isocloso*-$1\text{-}RhB_{10}H_8]$, crystals of which are orthorhombic, space group $P2_12_12_1$, with a = 1 267.5(3), b = 1 269.9(3), c = 1 683.4(3) pm, and Z = 4. In each compound the RhB_{10} cluster is a closed eleven-vertex deltahedron, the hexahapto borane–metal linkage being effected *via* one Rh–H–B and five Rh–B connectivities. The metal centre is an 18-electron d^6 rhodium(III) atom which can be thought to contribute four orbitals to the metallaborane cluster bonding scheme, thus inducing '*isocloso*' cluster character. The presence of a bridged metal–hydrogen–boron linkage on the closed polyhedral cluster is also notable.

It has previously been found that the reaction of the iridium(I) complex $[Ir(CO)Cl(PPh_3)_2]$ with the *closo*-$[B_{10}H_{10}]^{2-}$ anion in boiling methanol solution yields isomeric *nido* eleven-vertex cluster compounds of molecular formula $[(CO)(PPh_3)_2IrB_{10}H_{11}(PPh_3)]$,[1] together with a variety of metallaborane and metallacarborane degradation products which include six-vertex and ten-vertex species, and which include compounds with either one or two metal centres.[2–5] We now report that, by contrast, the reaction of the rhodium(III) complex $[RhCl_3(PMe_2Ph)_3]$ under the same conditions gives the new eleven-vertex species $[(PMe_2Ph)_2RhHB_{10}H_8(OMe)_2]$ (**1**) and $[(PMe_2Ph)_2RhHB_{10}H_8Cl(OMe)]$ (**2**). These have been characterized by single-crystal *X*-ray diffraction analysis and by n.m.r. spectroscopy, and each has an *isocloso* type configuration and electronic structure similar to that recently reported for a number of ruthenium and osmium complexes.[6–8] These eleven-vertex closed-cluster compounds pose interesting questions for the development of cluster bonding theory[6,7,9] and the two rhodium species reported here (which are also the first structurally characterized polyhedral rhodaboranes) throw additional light on the nature of the metal–borane bonding within this configuration.

Results and Discussion

The reaction between equimolar quantities of $[NEt_3H]_2[B_{10}H_{10}]$ and $[RhCl_3(PMe_2Ph)_3]$ in boiling methanol for 20 min, followed by thin-layer chromatographic separation of the reaction products, gave an air-stable bright orange-yellow crystalline compound, *isocloso*-$[(PMe_2Ph)_2RhHB_{10}H_8(OMe)_2]$, as the predominant metallaborane product in an isolable yield of 5%. Erratic yields (which appear to depend critically on the purity of the starting materials) of other metallaboranes were also obtained and one of these was found to be the related compound *isocloso*-$[(PMe_2Ph)_2RhHB_{10}H_8Cl(OMe)]$. The major product of the reaction was the nonaborane adduct $B_9H_{13}(PMe_2Ph)$ and there was no evidence for significant quantities of any rhodaborane products analogous to the wide variety of iridium-containing species formed in the related reaction between $[Ir(CO)Cl(PPh_3)_2]$ and *closo*-$[B_{10}H_{10}]^{2-}$ in methanol.[1–5] Conversely, however, the similarities between the n.m.r. properties of the two *closo* type rhodaboranes reported here and the n.m.r. properties of some of the yet unidentified components of the iridium reaction indicate that this latter may produce small amounts of iridaboranes with the same closed eleven-vertex configuration.

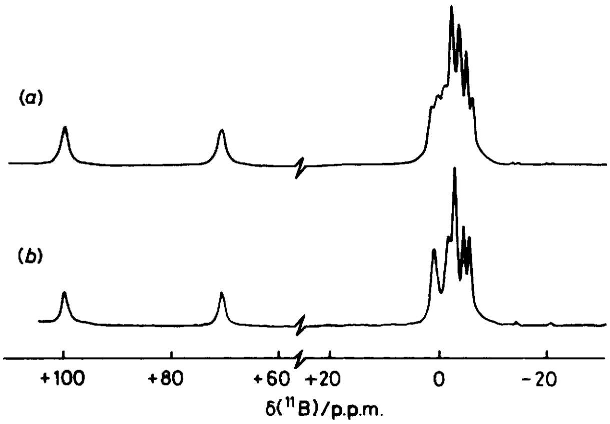

Figure 1. Boron-11 n.m.r. spectra of $[(PMe_2Ph)_2RhHB_{10}H_8(OMe)_2]$ recorded at 115.5 MHz ($CDCl_3$ solution): (*a*) the normal spectrum, (*b*) with ^1H broad-band noise decoupling

The high-field ^{11}B n.m.r. spectrum of $[(PMe_2Ph)_2RhHB_{10}H_8(OMe)_2]$ (Figure 1 and Table 1), when compared to those[7] of ruthenium species such as $[(PMe_2Ph)_2RuB_{10}H_8(OMe)_2]$, indicate an overall similar geometric and electronic cluster structure, although with an idealized C_s mirror plane rather than two-fold C_{2v} symmetry. This is confirmed by the results of single-crystal *X*-ray diffraction analysis: the unit cell was found to contain two independent molecules in which the principal difference, other than Rh–P and P–C bond rotation, was the

---

* 1,1-Bis(dimethylphenylphosphine)-1,2-μ-hydrido-2,5-dimethoxo-*isocloso*-1-rhodaundecaborane and 2-chloro-1,1-bis(dimethylphenylphosphine)-1,2-μ-hydrido-5-methoxo-*isocloso*-1-rhodaundecaborane respectively.

Supplementary data available (No. SUP 56405, 3 pp.): thermal parameters. See Instructions for Authors, *J. Chem. Soc., Dalton Trans.*, 1986, Issue 1, pp. xvii—xx. Structure factors are available from the editorial office.

Table 1. N.m.r. parameters for $[(PMe_2Ph)_2RhHB_{10}H_8(OMe)_2]$ and for $[(PMe_2Ph)_2RuB_{10}H_8(OMe)_2]$

	$[(PMe_2Ph)_2RhHB_{10}H_8(OMe)_2]$[a]			$[(PMe_2Ph)_2RuB_{10}H_8(OMe)_2]$[b]		
Tentative assignments[c]	$\delta(^{11}B)$/p.p.m.[d]	^{11}B relative intensity	$\delta(^1H)$/p.p.m.[e,f]	$\delta(^{11}B)$/p.p.m.[d,g]	^{11}B relative intensity	$\delta(^1H)$/p.p.m.[e,f]
(5) (2)	+99.9 +70.7[i]	1 1	+4.59 (OMe)[h] +4.41 (OMe)[h]	+90.1	2	+4.30 (OMe)
(9,11)	+0.7	2	+2.12	+3.6	2	+2.25
(3,4), (6,7)	−2.0 −3.1	2 1	+1.46 +1.52	+7.4	4	+2.41
(8,10)	−4.7 −5.8	1 1	+3.02 +3.00	+8.5	2	+3.72
(1)	*j*		−2.69[i,k]	*l*		
P-methyl[m]	*n*		+1.07[o,p] +1.26[o,q]	*r*		+1.15[s]

[a] CD_2Cl_2 solution at +22 °C. [b] $CDCl_3$ solution at +21 °C; data from ref. 22. [c] Numbering as in Figure 2. [d] To low field (high frequency) of $BF_3(OEt_2)$. [e] To low field (high frequency) of $SiMe_4$. [f] $\delta(^1H)$ related to corresponding directly bound $\delta(^{11}B)$ by ^1H-{^{11}B(selective)} experiments. [g] ^{11}B–^{11}B connectivities and thence assignments established and/or confirmed by 128-MHz ^{11}B–^{11}B COSY two-dimensional n.m.r. spectroscopy. [h] Selective sharpening of B-methoxy protons in ^1H-{^{11}B} experiments indicates small couplings $^3J(^{11}B–O–C–^1H)$ of $\leqslant$ *ca.* 2 Hz. [i] Selective sharpening of $\delta(^1H)$ −2.69 p.p.m. by irradiation at $\nu(^{11}B)$ corresponding to $\delta(^{11}B)$ +70.7 p.p.m.; $^nJ(^{11}B–^1H)$ of 55 ± 15 Hz present, probably due to $^1J(^{11}B–^1H)$ [Rh(1)–H–B(2) bridge] rather than $^2J(^{11}B–Rh–^1H)$(transoid) (see text). [j] Vertex (1) occupied by Rh. [k] Doublet [$^1J(^{103}Rh–^1H)$ *ca.* 14 Hz] of triplets [$^2J(^{31}P–Rh–^1H)$(*cis*) *ca.* 13 Hz] in ^1H-{^{11}B(broad band)} spectrum. [l] Vertex (1) occupied by Ru. [m] $[AX_n]_2$-type spin systems, X = ^1H, A = ^{31}P; intensity distribution corresponds to $|^2J(^{31}P–Rh–^{31}P)(cis)|$ of a few tens of Hz; $N = (^2J + {}^4J)(^{31}P–^1H)$ (see *p*, *q*, and *s*). [n] $\delta(^{31}P)$ −5.2 p.p.m. at −45 °C in $CDCl_3$; $^1J(^{103}Rh–^{31}P)$ 108 Hz. [o] Two chemically inequivalent P-methyl groups due to adjacent prochiral centre. [p] $N(^{31}P–^1H)$ 9.7 Hz. [q] $N(^{31}P–^1H)$ 9.5 Hz. [r] $\delta(^{31}P)$ −3.8 p.p.m. at −50 °C in $CDCl_3$. [s] $N(^{31}P–^1H)$ *ca.* 8 Hz.

Table 2. Interatomic distances (pm) for the two independent molecules of *isocloso*-$[(PMe_2Ph)_2RhHB_{10}H_8(OMe)_2]$

	Molecule A				Molecule B		
(*i*) To the rhodium atom							
Rh(1)–P(1)	235.5(4)	Rh(1)–P(2)	237.3(3)	Rh(1′)–P(1′)	236.0(3)	Rh(1′)–P(2′)	235.7(4)
Rh(1)–B(2)	222.0(8)	Rh(1)–B(5)	206.7(9)	Rh(1′)–B(2′)	222.1(7)	Rh(1′)–B(5′)	207.8(9)
Rh(1)–B(3)	230.4(7)	Rh(1)–B(6)	228.4(9)	Rh(1′)–B(3′)	230.5(7)	Rh(1′)–B(6′)	228.4(9)
Rh(1)–B(4)	230.0(8)	Rh(1)–B(7)	231.8(9)	Rh(1′)–B(4′)	229.4(9)	B(1′)–B(7′)	232.8(9)
Rh(1)–H(1,2)	181(2)			Rh(1′)–H(1′,2′)	173(2)		
(*ii*) Boron–boron							
B(2)–B(3)	194.9(11)	B(2)–B(7)	190.8(10)	B(2′)–B(3′)	185.4(12)	B(2′)–B(7′)	198.1(13)
B(2)–B(8)	177.4(11)	B(5)–B(10)	181.0(12)	B(2′)–B(8′)	178.8(12)	B(5′)–B(10′)	178.3(11)
B(3)–B(4)	168.2(11)	B(6)–B(7)	172.0(11)	B(3′)–B(4′)	172.3(11)	B(6′)–B(7′)	171.5(11)
B(3)–B(8)	177.9(12)	B(7)–B(8)	178.0(9)	B(3′)–B(8′)	177.8(11)	B(7′)–B(8′)	179.6(11)
B(3)–B(9)	175.1(12)	B(7)–B(11)	175.9(11)	B(3′)–B(9′)	175.8(13)	B(7′)–B(11′)	174.0(12)
B(4)–B(5)	187.6(10)	B(5)–B(6)	182.1(13)	B(4′)–B(5′)	181.9(11)	B(5′)–B(6′)	186.4(10)
B(4)–B(9)	173.6(12)	B(6)–B(11)	176.9(10)	B(4′)–B(9′)	177.4(10)	B(6′)–B(11′)	177.7(10)
B(4)–B(10)	182.0(13)	B(6)–B(10)	182.2(11)	B(4′)–B(10′)	181.1(12)	B(6′)–B(10′)	184.0(12)
B(8)–B(9)	177.7(12)	B(8)–B(11)	177.3(12)	B(8′)–B(9′)	176.3(12)	B(8′)–B(11′)	180.0(12)
B(9)–B(10)	175.7(11)	B(10)–B(11)	174.4(13)	B(9′)–B(10′)	176.6(11)	B(10′)–B(11′)	176.4(11)
B(9)–B(11)	175.5(12)			B(9′)–B(11′)	175.8(12)		
(*iii*) Boron–hydrogen							
B(2)–H(1,2)	132(2)			B(2′)–H(1′,2′)	144(2)		
B(3)–H(3)	109(2)	B(7)–H(7)	117(2)	B(3′)–H(3′)	120(2)	B(7′)–H(7′)	112(2)
B(4)–H(4)	121(2)	B(6)–H(6)	112(2)	B(4′)–H(4′)	108(2)	B(6′)–H(6′)	110(2)
B(8)–H(8)	119(2)	B(10)–H(10)	113(2)	B(8′)–H(8′)	110(2)	B(10′)–H(10′)	103(3)
B(9)–H(9)	102(1)	B(11)–H(11)	110(3)	B(9′)–H(9′)	96(2)	B(11′)–H(11′)	126(2)
(*iv*) Others							
B(2)–O(2)	137.2(8)	B(5)–O(5)	134.2(9)	B(2′)–O(2′)	137.1(9)	B(5′)–O(5′)	135.0(8)
O(2)–C(2)	138.3(8)	O(5)–C(5)	135.7(12)	O(2′)–C(2′)	140.7(8)	O(5′)–C(5′)	142.1(10)
P(1)–C(11)	182.5(7)	P(2)–C(21)	183.3(9)	P(1′)–C(11′)	181.3(9)	P(2′)–C(21′)	182.4(8)
P(1)–C(12)	180.7(8)	P(2)–C(22)	179.7(9)	P(1′)–C(12′)	180.7(10)	P(2′)–C(22′)	182.5(8)
P(1)–C(131)	179.5(5)	P(2)–C(231)	181.7(6)	P(1′)–C(131′)	179.5(5)	P(2′)–C(231′)	181.1(6)

orientation of the methoxy groups with respect to the B(2)–O(2) bond. A drawing of the two rotamers is given in Figure 2 and selected interatomic distances and angles are in Tables 2 and 3 respectively.

The n.m.r. data and *X*-ray diffraction results of the closely related derivative $[(PMe_2Ph)_2RhHB_{10}H_8Cl(OMe)]$ are in Tables 4 and 5, and Figure 3, and the Experimental section.

The geometries of all three crystallographically independent clusters [Figures 2(*a*), 2(*b*), and 3] are very similar so we discuss them as one except where specifically indicated. The gross

Table 3. Selected angles (°) between interatomic vectors for the two independent molecules of *isocloso*-$[(PMe_2Ph)_2RhHB_{10}H_8(OMe)_2]$

	Molecule A				Molecule B		
(*i*) About the rhodium atom							
P(1)–Rh(1)–P(2)	95.6(2)			P(1′)–Rh(1′)–P(2′)	95.2(2)		
P(1)–Rh(1)–B(2)	116.5(3)	P(2)–Rh(1)–B(2)	109.3(3)	P(1′)–Rh(1′)–B(2′)	104.9(3)	P(2′)–Rh(1′)–B(2′)	120.8(3)
P(1)–Rh(1)–B(3)	95.2(3)	P(2)–Rh(1)–B(2)	160.2(3)	P(1′)–Rh(1′)–B(3′)	92.2(3)	P(2′)–Rh(1′)–B(3′)	168.4(2)
P(1)–Rh(1)–B(4)	87.7(3)	P(2)–Rh(1)–B(4)	154.2(2)	P(1′)–Rh(1′)–B(4′)	91.8(3)	P(2′)–Rh(1′)–B(4′)	144.2(2)
P(1)–Rh(1)–B(5)	97.4(3)	P(2)–Rh(1)–B(5)	103.7(3)	P(1′)–Rh(1′)–B(5′)	106.6(3)	P(2′)–Rh(1′)–B(5′)	95.7(3)
P(1)–Rh(1)–B(6)	146.5(2)	P(2)–Rh(1)–B(6)	91.1(2)	P(1′)–Rh(1′)–B(6′)	157.0(2)	P(2′)–Rh(1′)–B(6′)	87.3(3)
P(1)–Rh(1)–B(7)	165.4(1)	P(2)–Rh(1)–B(7)	94.0(2)	P(1′)–Rh(1′)–B(7′)	156.4(2)	P(2′)–Rh(1′)–B(7′)	98.2(3)
B(2)–Rh(1)–B(3)	51.0(3)	B(2)–Rh(1)–B(7)	49.7(2)	B(2′)–Rh(1′)–B(3′)	48.3(2)	B(2′)–Rh(1′)–B(7′)	51.6(3)
B(2)–Rh(1)–B(4)	91.9(3)	B(2)–Rh(1)–B(6)	91.8(3)	B(2′)–Rh(1′)–B(4′)	90.8(3)	B(2′)–Rh(1′)–B(6′)	93.3(3)
B(2)–Rh(1)–B(5)	128.9(3)			B(2′)–Rh(1′)–B(5′)	128.4(3)		
B(3)–Rh(1)–B(4)	42.9(2)	B(6)–Rh(1)–B(7)	43.9(2)	B(3′)–Rh(1′)–B(4′)	44.0(2)	B(6′)–Rh(1′)–B(7′)	43.6(2)
B(3)–Rh(1)–B(5)	91.2(3)	B(5)–Rh(1)–B(7)	90.9(4)	B(3′)–Rh(1′)–B(5′)	90.7(4)	B(5′)–Rh(1′)–B(7′)	91.2(3)
B(3)–Rh(1)–B(6)	88.9(3)	B(4)–Rh(1)–B(7)	88.4(2)	B(3′)–Rh(1′)–B(6′)	89.3(3)	B(4′)–Rh(1′)–B(7′)	88.5(3)
B(3)–Rh(1)–B(7)	72.5(3)	B(4)–Rh(1)–B(6)	73.0(3)	B(3′)–Rh(1′)–B(7′)	71.9(3)	B(4′)–Rh(1′)–B(6′)	73.6(3)
B(4)–Rh(1)–B(5)	50.5(3)	B(5)–Rh(1)–B(6)	49.2(3)	B(4′)–Rh(1′)–B(5′)	48.9(2)	B(5′)–Rh(1′)–B(6′)	50.3(3)
(*ii*) Boron–boron–boron							
B(3)–B(2)–B(7)	90.3(5)	B(4)–B(5)–B(6)	95.1(5)	B(3′)–B(2′)–B(7′)	90.3(5)	B(4′)–B(5′)–B(6′)	96.2(5)
B(2)–B(3)–B(4)	126.7(6)	B(2)–B(7)–B(6)	126.2(6)	B(2′)–B(3′)–B(4′)	128.0(6)	B(2′)–B(7′)–B(6′)	124.7(6)
B(3)–B(4)–B(5)	123.0(6)	B(5)–B(6)–B(7)	124.2(6)	B(3′)–B(4′)–B(5′)	123.6(6)	B(5′)–B(6′)–B(7′)	123.5(6)
(*iii*) Others							
O(2)–B(2)–Rh(1)	154.0(4)	O(5)–B(5)–Rh(1)	130.0(6)	O(2′)–B(2′)–Rh(1′)	142.9(4)	O(5′)–B(5′)–Rh(1′)	130.3(5)
O(2)–B(2)–B(3)	129.6(5)	O(5)–B(5)–B(4)	130.4(6)	O(2′)–B(2′)–B(3′)	125.5(6)	O(5′)–B(5′)–B(4′)	131.9(5)
O(2)–B(2)–B(7)	124.9(5)	O(5)–B(5)–B(6)	132.3(5)	O(2′)–B(2′)–B(7′)	137.1(5)	O(5′)–B(5′)–B(6′)	130.0(6)
O(2)–B(2)–B(8)	109.2(5)	O(5)–B(5)–B(10)	126.5(7)	O(2′)–B(2′)–B(8′)	118.9(5)	O(5′)–B(5′)–B(10′)	126.2(7)
O(2)–B(2)–H(1,2)	100.2(11)			O(2′)–B(2′)–H(1′,2′)	94.7(11)		
B(2)–O(2)–C(2)	123.1(5)	B(5)–O(5)–C(5)	125.1(7)	B(2′)–O(2′)–C(2′)	124.0(6)	B(5′)–O(5′)–C(5′)	121.4(6)
Rh(1)–H(1,2)–B(2)	89.0(11)			Rh(1′)–H(1′,2′)–B(2′)	88.5(12)		

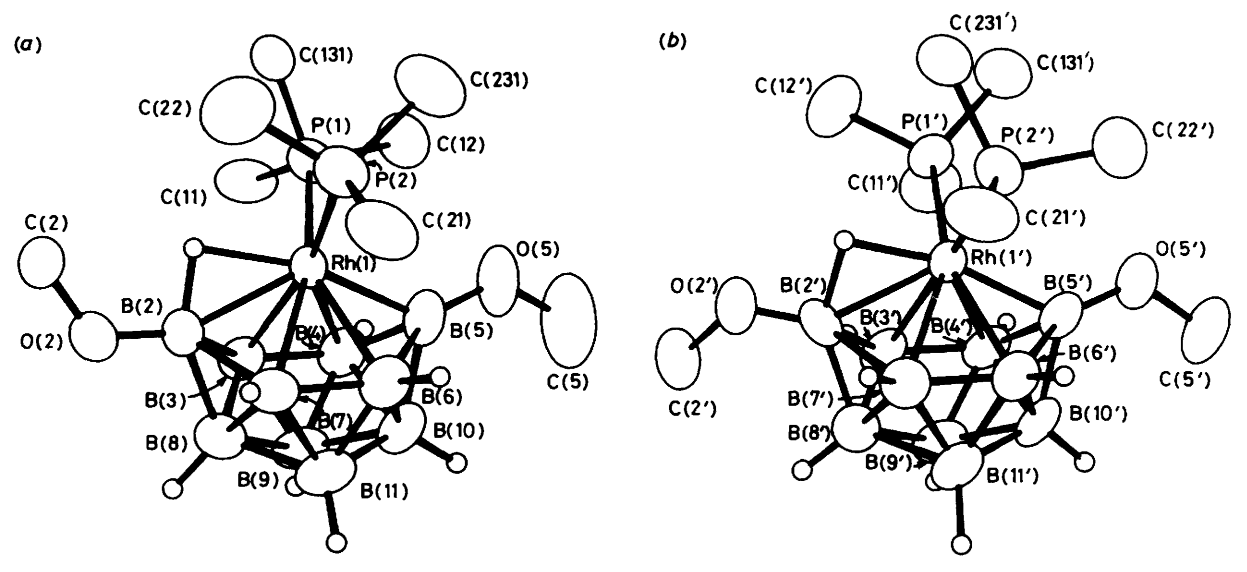

Figure 2. ORTEP drawings of the crystallographically determined molecular structure of $[(PMe_2Ph)_2RhHB_{10}H_8(OMe)_2]$, with selected organyl atoms omitted for clarity. The crystal contains two distinct molecular bond-rotamer configurations: (*a*) molecule A, (*b*) molecule B

molecular cluster structure can be seen to be that of an open *nido/arachno* ten-vertex decaboranyl cluster fragment with the boat open face capped by the metal atom, resulting in a hexahapto borane–metal linkage. The distances B(3)–B(4) and B(6)–B(7), which average at less than 170 pm, are much shorter than the corresponding diagnostically long distances of 197 pm in *nido*-decaborane itself.[10] This indicates that the ten-boron fragment does not have the straightforward *nido*-decaboranyl properties of a direct *nido*-$B_{10}H_{14}$ derivative (see discussion below), which is also indicated by the boron-11 n.m.r. shielding behaviour of the cluster (Table 1). This shielding behaviour is again substantially different from that of $B_{10}H_{14}$ itself, and also indeed different from that of *arachno*-decaboranyl ten-vertex clusters.[11–13]

Table 4. Interatomic distances (pm) for *isocloso*-$[(PMe_2Ph)_2RhHB_{10}H_8Cl(OMe)]$

(*i*) To the rhodium atom			
Rh(1)–P(1)	235.6(4)	Rh(1)–P(2)	236.3(4)
Rh(1)–B(2)	217.6(9)	Rh(1)–B(5)	206.9(9)
Rh(1)–B(3)	231.6(10)	Rh(1)–B(6)	225.7(10)
Rh(1)–B(4)	230.2(9)	Rh(1)–B(7)	228.6(9)
Rh(1)–H(1,2)	165.9(29)		
(*ii*) Boron–boron			
B(2)–B(3)	184.3(13)	B(2)–B(7)	189.7(14)
B(2)–B(8)	176.4(12)	B(5)–B(10)	180.8(11)
B(3)–B(4)	174.0(17)	B(6)–B(7)	169.9(17)
B(3)–B(8)	178.9(14)	B(7)–B(8)	183.0(14)
B(3)–B(9)	178.7(15)	B(7)–B(11)	176.8(14)
B(4)–B(5)	185.8(14)	B(5)–B(6)	184.8(14)
B(4)–B(9)	174.8(15)	B(6)–B(11)	175.8(15)
B(4)–B(10)	182.0(14)	B(6)–B(10)	180.6(14)
B(8)–B(9)	177.0(16)	B(8)–B(11)	177.0(17)
B(9)–B(10)	174.7(17)	B(10)–B(11)	175.5(15)
B(9)–B(11)			
(*iii*) Boron–hydrogen			
B(2)–H(1,2)	128(2)		
B(3)–H(3)	105(2)	B(7)–H(7)	116(2)
B(4)–H(4)	118(3)	B(6)–H(6)	116(3)
B(8)–H(8)	117(3)	B(10)–H(10)	107(3)
B(9)–H(9)	113(2)	B(11)–H(11)	106(2)
(*iv*) Others			
B(2)–Cl(2)	181.2(10)	B(5)–O(5)	136.2(9)
P(1)–C(11)	183.1(8)	P(2)–C(21)	179.8(10)
P(1)–C(12)	183.3(10)	P(2)–C(22)	182.1(8)
P(1)–C(131)	180.1(6)	P(2)–C(231)	182.5(6)

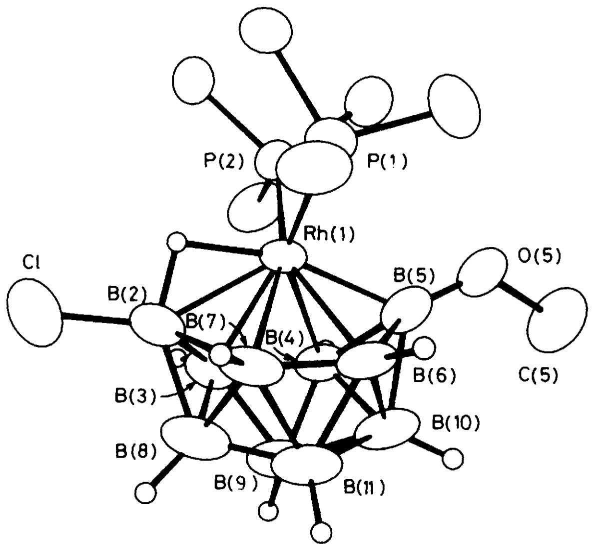

Figure 3. ORTEP drawing of the crystallographically determined molecular structure of $[(PMe_2Ph)_2RhHB_{10}H_8Cl(OMe)]$

Table 5. Selected angles (°) between interatomic vectors for *isocloso*-$[(PMe_2Ph)_2RhHB_{10}H_8Cl(OMe)]$

(*i*) About the rhodium atom			
P(1)–Rh(1)–P(2)	94.1(2)		
P(1)–Rh(1)–B(2)	116.1(3)	P(2)–Rh(1)–B(2)	115.0(3)
P(1)–Rh(1)–B(3)	164.1(2)	P(2)–Rh(1)–B(3)	96.3(3)
P(1)–Rh(1)–B(4)	147.9(3)	P(2)–Rh(1)–B(4)	89.8(3)
P(1)–Rh(1)–B(5)	98.0(3)	P(2)–Rh(1)–B(5)	98.6(3)
P(1)–Rh(1)–B(6)	87.8(3)	P(2)–Rh(1)–B(6)	148.7(3)
P(1)–Rh(1)–B(7)	94.3(3)	P(2)–Rh(1)–B(7)	165.2(3)
B(2)–Rh(1)–B(3)	48.3(3)	B(2)–Rh(1)–B(6)	91.7(4)
B(2)–Rh(1)–B(4)	90.6(4)	B(2)–Rh(1)–B(7)	50.2(4)
B(1)–Rh(1)–B(5)	128.5(4)		
B(3)–Rh(1)–B(4)	44.3(4)	B(6)–Rh(1)–B(7)	43.9(4)
B(3)–Rh(1)–B(5)	92.3(4)	B(5)–Rh(1)–B(7)	92.2(4)
B(3)–Rh(1)–B(6)	89.4(4)	B(4)–Rh(1)–B(7)	89.5(4)
B(3)–Rh(1)–B(7)	73.0(3)	B(4)–Rh(1)–B(6)	73.1(3)
B(4)–Rh(1)–B(5)	50.0(4)	B(5)–Rh(1)–B(6)	50.3(4)
(*ii*) Boron–boron			
B(3)–B(2)–B(7)	94.2(6)	B(4)–B(5)–B(6)	94.2(6)
B(2)–B(3)–B(4)	125.4(7)	B(2)–B(7)–B(6)	124.4(7)
B(3)–B(4)–B(5)	123.2(7)	B(5)–B(6)–B(7)	124.7(7)
(*iii*) Others			
Cl(2)–B(2)–Rh(1)	146.7(4)	O(5)–B(5)–Rh(1)	130.7(4)
Cl(2)–B(2)–B(3)	129.1(7)	O(5)–B(5)–B(4)	131.3(7)
Cl(2)–B(2)–B(7)	127.3(6)	O(5)–B(5)–B(6)	132.2(7)
Cl(2)–B(2)–B(8)	113.2(6)	O(5)–B(5)–B(10)	126.7(6)
Cl(2)–B(2)–H(1,2)	97.3(14)	O(5)–B(5)–C(5)	122.2(6)
B(2)–H(1,2)–Rh(1)	94.6(15)		

That the electronic structure of the RhB_{10} cluster conforms to idealized C_s symmetry, rather than the idealized C_{2v} symmetry exhibited by the previously described ruthenium analogue,[6,7] arises from the presence of a rhodium-bound hydrogen on the plane containing Rh(1) and the two substituted boron atoms B(2) and B(5). The crystallographic results show that this has a Rh(1)–H–B(2) bridging configuration, rather than Rh(1)–H terminal, which is consistent with the n.m.r. behaviour (Table 1): although the novelty of the bonding configuration means that the criteria for n.m.r. behaviour are not established, the incidence and magnitude of the coupling $^nJ(^{11}B-^1H)$ to this hydride of *ca.* 50 Hz probably favours a one-bond $^1J(^{11}B-^1H)$ [Rh–H–B(2) bridge] coupling rather than a transoid coupling $^2J[^{11}B(5)-Rh-^1H(terminal)]$, and the couplings $^1J(^{103}Rh-^1H)$ and $^2J(^{31}P-Rh-^1H)$ (*cis*) of 12—13 Hz are perhaps smaller than would be expected for straightforward terminal rhodium–hydride behaviour.

There is only a slight tilt of the Rh(1)P(1)P(2) bonding plane away from this hydride position [dihedral angle Rh(1)P(1)-P(2)/Rh(1)B(9)B(11) *ca.* 13° for the methoxochloro compound], which indicates that the P(1)P(2)H(1,2-bridge) bonding disposition is not trigonal about the idealized C_s axis of the RhB_{10} unit, but approximates more closely to RhP(1)P(2) digonal in the Rh(1)B(9)B(11) plane containing the C_2 axis. If the closed nature of the cluster implies a *closo* electron count,[6,7] then the neutral $Rh(PMe_2Ph)_2H$ centre is required to contribute four electrons to the cluster scheme. The atomic dispositions then suggest that this is achieved *via* an octahedral 18-electron d^6 rhodium(III) configuration with a four-orbital involvement in the cluster bonding scheme, structure (**I**), the four electrons being formally supplied by the two electrons in the Rh–H bond of the neutral $Rh(PMe_2Ph)_2H$ unit, together with two straightforward metal valence electrons. Significant contributions to the metal–borane bonding will then presumably occur *via* three, three-centre bonds, Rh(1)H(1,2-bridge)-B(2), Rh(1)B(3)B(4), and Rh(1)B(6)B(7), together with a two-centre bond, Rh(1)B(5).

Apart from the tilt of the Rh(1)P(1)P(2) plane relative to the C_2 axis of an idealized C_{2v} B_{10} configuration, there are other noteworthy cluster distortions attributable to the presence of the bridging hydrogen atom. First, the bridged rhodium–boron distance Rh(1)–B(2) is significantly longer than Rh(1)–B(5); this

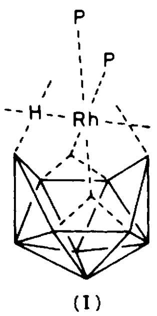

(I)

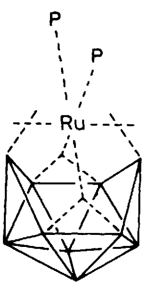

(II)

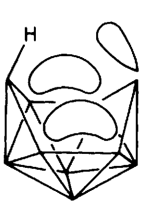

(III)

could be regarded partly as a consequence of the tilt, but also concomitantly as a result of the conversion of a (hypothetical) M(1)–B(2) two-electron, two-centre bond [*e.g.* as in structure **(II)**] to a three-centre M(1)–H(1,2)–B(2) linkage, structure **(I)**. For example, in binary boron hydride chemistry, otherwise similar hydrogen-bridged *versus* unbridged two-electron interboron links commonly differ by up to 20 pm or so.[14] Second, the interboron distances B(2)–B(3) and B(2)–B(7) to the hydrogen-bridged boron atom B(2) appear to be somewhat longer than the corresponding positions at the unbridged end of the molecule, and also longer than those in totally unbridged species such as $[(PPh_3)_2RuB_{10}H_8(OEt)_2]$.[6] One explanation of this could involve a reduced electron density in these linkages, the withdrawal arising from the presence of the proton in the Ru(1)–B(2) bonding link. These particular interboron distances are in any event long (presumably, in the known unbridged species, indicating a weaker bonding interaction) and therefore would be particularly susceptible to small changes in electron density; in this context, therefore, as yet unquantified bonding factors associated with the Cl (*versus* OMe) ligand in $[(PMe_2Ph)_2RhHB_{10}H_8Cl(OMe)]$ may have to be invoked to account for the diminished lengthening observed for this species, although in this case the possibility of some crystallographic disorder can not be rigorously discounted as the Cl atom shows slightly higher thermal parameters than might be normally expected. It is in any event interesting that it is the chlorinated atom B(2) which has the hydrogen bridge rather than the alkoxo-substituted B(5); the n.m.r. data show that this distinction remains in solution.

The incidence of a bridging hydrogen atom on a closed metallaborane cluster is rare, although several instances in metallacarbaborane chemistry are recognised[15] and it is known that $[B_{10}H_{10}]^{2-}$ can readily be protonated in reasonably acidic solutions.[16] As far as we are aware in formal metallaborane chemistry, however, the only substantiated instances are in the polymetallic species *isocloso*-$[(CO)_{12}HFe_4BH_2]$,[17] *isocloso*-$[(CO)_{12}HRu_4BH_2]$,[18] *closo*-$[(\eta^5\text{-}C_5H_5)_3Co_3B_3H_5]$,[19] and *closo*-$[(\eta^5\text{-}C_5H_5)_2Co_2B_4H_6]$ (together with its alkyl-substituted derivatives).[20] A species tentatively formulated as $[(\eta^5\text{-}C_5H_5)CoB_{10}H_{12}]$[21] would also in principle be in this category but this has not yet been structurally characterized. This rarity is perhaps surprising, since, for a given structural type, it is the incidence of bridging hydrogen atoms in metallacarbaboranes that is expected to be proportionately the rarer. This arises because, in the metallacarbaboranes, the excess electrons, over the nominal $2n$, that are required for a stable cluster electron count are supplied by having carbon instead of (boron + hydrogen), and so the presence of bridging hydrogen atoms to supply electrons is less necessary (for the given structural type). The relative incidences therefore probably reflect the types and volume of chemistry that happen to have been studied within the two general areas.

In terms of a metal complex of a polydentate borane ligand,[9] the (as yet unsynthesized) unsubstituted parent compound $[(PMe_2Ph)_2RhHB_{10}H_{10}]$ would be a notional complex between the ten-electron rhodium(III) centre $[Rh(PMe_2Ph)_2]^{3+}$ and the quadridentate hexahapto ligand $[B_{10}H_{11}]^{3-}$ [structure **(III)**]; this last entity can be regarded as being formally derived from the triple deprotonation of what would be an excited-state *nido*-$B_{10}H_{14}$ configuration of *styx* 2802 topology rather than the configuration of *styx* 4620 topology that is in fact exhibited by (ground-state) $B_{10}H_{14}$ itself.

These considerations lend additional support to the similar conclusions made about the metal–borane bonding in the recently reported compounds $[(PR_3)_2MB_{10}H_8(OR')_2]$ (M = Ru or Os, PR_3 = PMe_2Ph or PPh_3, R′ = Me or Et),[6,7,22] which have similar cluster n.m.r. properties to the rhodium compounds (*e.g.* Table 1), and therefore similar cluster electronic structures. These ruthenium and osmium species are also believed to have an essentially octahedral metal bonding-orbital configuration with a four-orbital, four-electron contribution from the metal centre to the cluster bonding scheme [structure **(II)**], but within the constraints of an overall 16-electron d^4 metal configuration, rather than the 18-electron d^6 one of the rhodium species reported here. The cluster electronic structures of the rhodium and ruthenium species are related by a notional protonation $\rightleftharpoons$ deprotonation of the two-electron metal–B(2) bond [*cf.* structures **(I)** and **(II)**]. The four-orbital involvement of the metal centres with the intracluster bonding, rather than the three-orbital involvement implied in classical cluster bonding theory, merits the descriptor '*isocloso*' for these species rather than '*closo*'.[6] It happens that in eleven-vertex clusters the *closo* and *isocloso* configurations have similar gross geometries;[6,7] in nine-vertex and ten-vertex metallaborane chemistry this is not the case, and markedly different *isocloso* compared with *closo* geometries result.[7,23–25]

Experimental

General preparative and separatory techniques, and conditions for n.m.r. experiments, have been described elsewhere recently.[7,26]

Preparation of $[(PMe_2Ph)_2RhHB_{10}H_8(OMe)_2]$ **(1)** *and* $[(PMe_2Ph)_2RhHB_{10}H_8Cl(OMe)]$ **(2)**.—$[RhCl_3(PMe_2Ph)_3]$[27] (1.14 g, 3.63 mmol) and $[NEt_3H]_2[B_{10}H_{10}]$[28,29] (0.8 g, 2.48 mmol) were heated in MeOH (50 cm^3) under reflux in an atmosphere of dry nitrogen for 20 min; during this time the orange suspension turned to a dark red solution. The methanol was removed under reduced pressure at *ca.* 50 °C; the solid residue was dissolved in CH_2Cl_2 (5 cm^3) and the components separated and purified by repeated preparative-scale t.l.c. on silica, using dichloromethane–light petroleum (b.p. 60—80 °C) (70:30) as eluant. The first band, of R_f *ca.* 0.6, was not always present but on occasion was obtained in *ca.* 2% yield (20 mg); its yield was not increased by conducting the reaction in the presence of HCl. It was identified by *X*-ray crystallography, as $[(PMe_2Ph)_2RhHB_{10}H_8Cl(OMe)]$. At 32 MHz the compound had approximate $\delta(^{11}B)$ n.m.r. values ($CDCl_3$ solution) of −103 (1 B), −78 (1 B), +10 (2 B), +3 (4 B), and −2 p.p.m. (2 B) (*cf.* Table 1). The second band, of R_f *ca.* 0.4, was orange and was identified by multielement n.m.r. spectroscopy and *X*-ray crystallography as $[(PMe_2Ph)_2RhHB_{10}H_8(OMe)_2]$ (43 mg, 5% yield). Substantial quantities of a further rhodaborane, unstable under the preparative and separatory conditions used, were also present, as were the colourless phosphaboranes $BH_3(PMe_2Ph)$ and $B_9H_{13}(PMe_2Ph)$, both identified by n.m.r. spectroscopy.[26]

X-*Ray Studies*.—Intensity data for both compounds were collected on a Syntex $P2_1$ diffractometer operating in the ω—2θ scan mode using graphite-monochromatised Mo-K_α radiation (λ = 71.069 pm) following a standard procedure.[30] The data

Table 6. Atom co-ordinates (× 10^4) for (**1**)

Atom	*x*	*y*	*z*	Atom	*x*	*y*	*z*
Rh(1)	4 579	2 291	8 409	B(6)	3 847(7)	3 412(4)	8 056(4)
Rh(1′)	4 577	2 437	3 402	B(7)	4 295(6)	2 775(4)	7 318(3)
P(1)	4 631(2)	1 468(1)	9 301(1)	B(8)	2 765(6)	1 957(4)	6 852(4)
P(2)	7 009(2)	3 071(1)	8 878(1)	B(9)	1 395(6)	2 111(4)	7 381(4)
P(1′)	4 856(2)	2 665(1)	4 720(1)	B(10)	1 925(7)	3 057(4)	8 064(4)
P(2′)	7 029(2)	2 353(1)	3 391(1)	B(11)	2 520(7)	2 974(4)	7 217(4)
C(11)	3 434(6)	437(4)	8 961(4)	B(2′)	2 784(6)	1 317(4)	2 943(4)
C(12)	4 046(7)	1 862(4)	10 156(3)	B(3′)	2 072(6)	2 270(4)	3 229(4)
C(131)	6 353(3)	1 209(2)	9 614(2)	B(4′)	2 934(7)	3 291(4)	3 337(4)
C(132)	6 878(3)	641(2)	9 124(2)	B(5′)	4 747(7)	3 600(4)	3 151(3)
C(133)	8 266(3)	485(2)	9 339(2)	B(6′)	4 474(7)	2 783(4)	2 267(3)
C(134)	9 129(3)	897(2)	10 043(2)	B(7′)	3 567(7)	1 774(4)	2 150(3)
C(135)	8 604(3)	1 465(2)	10 533(2)	B(8′)	1 717(6)	1 722(4)	2 271(4)
C(136)	7 216(3)	1 621(2)	10 318(2)	B(9′)	1 606(7)	2 778(4)	2 509(4)
C(21)	7 472(6)	4 009(4)	8 526(4)	B(10′)	3 174(7)	3 466(4)	2 428(4)
C(22)	8 285(6)	2 473(5)	8 561(5)	B(11′)	2 595(7)	2 465(4)	1 819(4)
C(231)	7 670(4)	3 476(2)	9 884(2)	O(2)	4 792(4)	1 145(3)	6 644(2)
C(232)	9 078(4)	3 452(2)	10 233(2)	C(2)	6 000(6)	790(4)	6 752(4)
C(233)	9 578(4)	3 800(2)	11 001(2)	O(5)	3 430(5)	3 473(3)	9 578(3)
C(234)	8 671(4)	4 171(2)	11 421(2)	C(5)	2 581(9)	4 006(6)	9 812(5)
C(235)	7 263(4)	4 195(2)	11 072(2)	O(2′)	2 241(4)	547(2)	3 050(3)
C(236)	6 763(4)	3 847(2)	10 304(2)	C(2′)	755(6)	147(4)	2 834(4)
C(11′)	3 511(7)	3 142(5)	5 134(3)	O(5′)	5 794(5)	4 301(2)	3 431(2)
C(12′)	4 668(7)	1 683(4)	4 995(4)	C(5′)	5 728(8)	5 031(4)	3 159(4)
C(131′)	6 532(3)	3 310(2)	5 327(2)	H(1,2)	5 233(13)	1 511(13)	7 802(12)
C(132′)	7 043(3)	4 083(2)	5 186(2)	H(3)	2 341(13)	758(13)	7 467(12)
C(133′)	8 312(3)	4 608(2)	5 643(2)	H(4)	1 433(13)	1 786(13)	8 729(12)
C(134′)	9 070(3)	4 360(2)	6 242(2)	H(6)	4 471(13)	4 070(12)	8 297(12)
C(135′)	8 559(3)	3 587(2)	6 384(2)	H(7)	5 272(13)	3 054(13)	7 071(12)
C(136′)	7 290(3)	3 062(2)	5 926(2)	H(8)	2 329(14)	1 739(13)	6 241(13)
C(21′)	7 278(6)	1 744(4)	2 508(3)	H(9)	308(13)	1 874(12)	7 163(12)
C(22′)	8 348(6)	3 323(4)	3 508(4)	H(10)	1 113(13)	3 444(13)	8 231(12)
C(231′)	7 849(3)	1 821(4)	4 058(2)	H(11)	2 045(14)	3 337(13)	6 841(13)
C(232′)	8 972(3)	2 250(2)	4 667(2)	H(1,2′)	4 235(14)	1 376(13)	3 357(13)
C(233′)	9 586(3)	1 823(2)	5 169(2)	H(3′)	1 314(13)	2 148(13)	3 670(12)
C(234′)	9 077(3)	967(2)	5 062(2)	H(4′)	2 901(14)	3 748(13)	3 830(12)
C(235′)	7 954(3)	539(2)	4 452(2)	H(6′)	5 393(13)	2 929(12)	1 989(12)
C(236′)	7 339(3)	966(2)	3 950(2)	H(7′)	3 965(13)	1 216(13)	1 879(12)
B(2)	4 356(6)	1 627(4)	7 220(3)	H(8′)	766(13)	1 235(12)	1 957(12)
B(3)	2 546(6)	1 438(4)	7 586(4)	H(9′)	658(13)	2 913(12)	2 398(12)
B(4)	2 084(6)	2 066(4)	8 296(4)	H(10′)	3 037(14)	3 959(13)	2 193(13)
B(5)	3 318(7)	3 069(4)	8 863(4)	H(11′)	2 079(14)	2 386(13)	1 133(13)

Table 7. Atom co-ordinates (× 10^4) for (**2**)

Atom	*x*	*y*	*z*	Atom	*x*	*y*	*z*
Rh(1)	2 585	2 079	3 577	B(2)	2 617(7)	2 465(5)	4 836(4)
P(1)	1 231(1)	931(2)	3 165(1)	B(3)	3 644(6)	3 210(7)	4 304(6)
P(2)	3 956(1)	957(1)	3 144(1)	B(4)	3 622(6)	3 520(6)	3 296(6)
Cl(1)	2 625(3)	1 970(2)	5 846(1)	B(5)	2 551(7)	3 093(5)	2 615(4)
C(11)	−54(5)	1 188(5)	3 624(5)	B(6)	1 481(7)	3 431(6)	3 316(6)
C(12)	919(6)	925(7)	2 102(4)	B(7)	1 485(6)	3 135(6)	4 300(6)
C(131)	1 406(3)	−432(3)	3 429(3)	B(8)	2 561(8)	3 851(6)	4 784(5)
C(132)	1 419(3)	−1 251(3)	2 876(3)	B(9)	3 201(8)	4 473(7)	3 976(8)
C(133)	1 538(5)	−2 289(3)	3 132(3)	B(10)	2 503(8)	4 373(5)	3 084(5)
C(134)	1 644(3)	−2 509(3)	3 940(3)	B(11)	1 833(7)	4 422(7)	3 996(7)
C(135)	1 631(3)	−1 690(3)	4 492(3)	O(5)	2 553(5)	2 892(3)	1 820(3)
C(136)	1 512(3)	−652(3)	4 237(3)	C(5)	2 545(9)	3 711(6)	1 246(4)
C(21)	3 875(6)	548(6)	2 123(4)	H(1,2)	2 524(18)	1 575(17)	4 485(16)
C(22)	5 295(5)	1 466(6)	3 231(5)	H(3)	4 398(17)	3 041(17)	4 536(16)
C(231)	4 105(3)	−265(3)	3 702(2)	H(4)	4 496(17)	3 452(17)	3 061(17)
C(232)	4 027(3)	−1 251(3)	3 341(2)	H(6)	728(17)	3 406(17)	2 929(16)
C(233)	4 184(3)	−2 163(3)	3 788(2)	H(7)	764(16)	2 834(17)	4 660(16)
C(234)	4 419(3)	−2 089(3)	4 595(2)	H(8)	2 403(17)	4 284(17)	5 386(16)
C(235)	4 497(3)	−1 103(3)	4 956(2)	H(9)	3 755(17)	5 131(17)	4 140(16)
C(236)	4 340(3)	−192(3)	4 510(2)	H(10)	2 354(18)	4 940(17)	2 632(16)
				H(11)	1 415(17)	5 129(17)	4 112(16)

sets for both compounds were corrected for absorption empirically.[31] Both compounds were solved *via* standard heavy-atom techniques and refined by full-matrix least-squares [for compound (**1**) in two blocks, one molecule per block], using the SHELX program system.[32] Refinement for both compounds was essentially the same with all non-hydrogen atoms assigned anisotropic thermal parameters and phenyl groups included in refinement as rigid bodies with idealised hexagonal geometry (C–C 139.5 pm). All phenyl and methyl hydrogen atoms were included in calculated positions using AFIX routines in the SHELX program (C–H 108 pm) and were assigned an overall isotropic thermal parameter for each group. All other hydrogen atoms were located experimentally and were freely refined with individual isotropic thermal parameters. For the methoxochloro compound (**2**), unit weights were applied throughout while for the dimethoxo compound (**1**), the weighting scheme $w = 1/[\sigma^2(F_o) + g(F_o)^2]$ was used in which the parameter g was included in refinement to give a flat analysis of variance with increasing $\sin\theta$ and $(F/F_{max.})^{\frac{1}{2}}$. Atomic co-ordinates for compounds (**1**) and (**2**) are given in Tables 6 and 7 respectively.

Crystal data for compound (**1**). $C_{18}H_{37}B_{10}O_2P_2Rh$, M = 558.44, triclinic, a = 948.8(4), b = 1 675.5(6), c = 1 855.0(6) pm, α = 101.48(3), β = 99.55(3), γ = 99.82(3)°, U = 2.786 nm^3, Z = 4, space group $P\bar{1}$, D_c = 1.33 g cm^{-3}, μ = 6.63 cm^{-1}, $F(000)$ = 1 152.

Data collection. Scans running from 1° below $K_{\alpha1}$ to 1° above $K_{\alpha2}$, scan speeds 2.0—29.3° min^{-1}, $4.0 < 2\theta < 45.0°$. 7 317 Unique reflections, 6 764 observed [$I > 1.5\sigma(I)$], T = 290 K.

Structure refinement. Number of parameters 688, weighting factor g = 0.0001, R = 0.0472, R' = 0.0534.

Crystal data for compound (**2**). $C_{17}H_{34}B_{10}ClOP_2Rh$, M = 562.88, orthorhombic, a = 1 267.5(3), b = 1 269.9(3), c = 1 683.4(3) pm, U = 2.710 nm^3, Z = 4, space group $P2_12_12_1$, D_c = 1.27 g cm^{-3}, μ = 7.71 cm^{-1}, $F(000)$ = 1 144.

Data collection. Parameters as for (**1**). 2 651 Unique reflections, 2 527 observed [$I > 1.5\sigma(I)$].

Structure refinement. Number of parameters 323, unit weights, R = 0.0348.

Acknowledgements

We thank the S.E.R.C. for support and Dr. D. Reed (University of Edinburgh) for services in high-field n.m.r. spectroscopy.

References

1 J. E. Crook, N. N. Greenwood, and J. D. Kennedy, unpublished work.

2 J. E. Crook, Ph.D. Thesis, University of Leeds, 1982, and unpublished work.

3 J. E. Crook, N. N. Greenwood, J. D. Kennedy, and W. S. McDonald, *J. Chem. Soc., Chem. Commun.*, 1981, 933.

4 J. E. Crook, N. N. Greenwood, J. D. Kennedy, and W. S. McDonald, *J. Chem. Soc., Chem. Commun.*, 1982, 383.

5 J. E. Crook, N. N. Greenwood, J. D. Kennedy, and W. S. McDonald, *J. Chem. Soc., Chem. Commun.*, 1983, 83.

6 J. E. Crook, M. Elrington, N. N. Greenwood, J. D. Kennedy, and J. D. Woollins, *Polyhedron*, 1984, 3, 901.

7 J. E. Crook, M. Elrington, N. N. Greenwood, J. D. Kennedy, M. Thornton-Pett, and J. D. Woollins, *J. Chem. Soc., Dalton Trans.*, 1985, 2407.

8 M. Elrington, N. N. Greenwood, J. D. Kennedy, and M. Thornton-Pett, *J. Chem. Soc., Chem. Commun.*, 1984, 1398.

9 J. D. Kennedy, *Prog. Inorg. Chem.*, 1984, **32**, 591 and unpublished work.

10 A. Tippe and W. C. Hamilton, *Inorg. Chem.*, 1969, **8**, 464 and refs. therein.

11 M. A. Beckett and J. D. Kennedy, *J. Chem. Soc., Chem. Commun.*, 1983, 275.

12 J. D. Kennedy, in 'NMR in Inorganic and Organometallic Chemistry,' ed. J. Mason, Plenum, New York, in the press.

13 J. E. Crook, N. N. Greenwood, J. D. Kennedy, and W. S. McDonald, *J. Chem. Soc., Dalton Trans.*, 1984, 2487.

14 L. Barton, *Top. Curr. Chem.*, 1982, **100**, 169.

15 R. N. Grimes, in 'Metal Interactions with Boron Clusters,' ed. R. N. Grimes, Plenum, New York, 1982, p. 269; R. N. Grimes, in 'Comprehensive Organometallic Chemistry,' eds. G. Wilkinson, F. G. A. Stone, and E. W. Abel, Pergamon, Oxford, 1982, vol. 1, p. 459.

16 P. A. Wegner, D. M. Adams, F. J. Callabretta, L. T. Spada, and R. G. Unger, *J. Am. Chem. Soc.*, 1973, **95**, 7513.

17 K. S. Wong, W. R. Scheidt, and T. P. Fehlner, *J. Am. Chem. Soc.*, 1982, **104**, 1111.

18 C. R. Eady, B. F. G. Johnson, and J. Lewis, *J. Chem. Soc., Dalton Trans.*, 1977, 477.

19 J. R. Pipal and R. N. Grimes, *Inorg. Chem.*, 1977, **16**, 3255.

20 J. R. Pipal and R. N. Grimes, *Inorg. Chem.*, 1979, **18**, 252.

21 G. J. Zimmerman, L. W. Hall, and L. G. Sneddon, *Inorg. Chem.*, 1980, **19**, 3642.

22 M. Elrington, Ph.D. Thesis, University of Leeds, 1985, and unpublished work.

23 J. Bould, Ph.D. Thesis, University of Leeds, 1983.

24 J. Bould, J. E. Crook, N. N. Greenwood, J. D. Kennedy, and W. S. McDonald, *J. Chem. Soc., Chem. Commun.*, 1982, 346.

25 J. Bould, N. N. Greenwood, J. D. Kennedy, and W. S. McDonald, *J. Chem. Soc., Chem. Commun.*, 1982, 465.

26 M. J. Hails, N. N. Greenwood, J. D. Kennedy, and W. S. McDonald, *J. Chem. Soc., Dalton Trans.*, 1985, 953.

27 P. R. Brookes and B. L. Shaw, *J. Chem. Soc. A*, 1967, 1079.

28 M. F. Hawthorne and A. R. Pittochelli, *J. Am. Chem. Soc.*, 1959, **81**, 5519.

29 M. F. Hawthorne, R. L. Pilling, and R. N. Grimes, *J. Am. Chem. Soc.*, 1964, **86**, 5338.

30 A. Modinos and P. Woodward, *J. Chem. Soc., Dalton Trans.*, 1981, 1415.

31 N. Walker and P. Stuart, *Acta Crystallogr., Sect. A*, 1983, **39**, 158.

32 G. M. Sheldrick, SHELX 76, Program system for *X*-ray structure determination, University of Cambridge, 1976.

Received 17th April 1985; *Paper* 5/637